Therapeutic inhibition of the miR-34 family attenuates pathological cardiac remodeling and improves heart function

Bianca C. Bernardo[a], Xiao-Ming Gao[a,1], Catherine E. Winbanks[a,1], Esther J. H. Boey[a], Yow Keat Tham[a], Helen Kiriazis[a], Paul Gregorevic[a], Susanna Obad[b], Sakari Kauppinen[b,c], Xiao-Jun Du[a], Ruby C. Y. Lin[d], and Julie R. McMullen[a,2]

[a]Baker IDI Heart and Diabetes Institute, Melbourne, VIC 8008, Australia; [b]Santaris Pharma, 2970 Horsholm, Denmark; [c]Aalborg University Copenhagen, 2450 Copenhagen SV, Denmark; and [d]Ramaciotti Centre for Gene Function Analysis, University of New South Wales, Randwick, NSW 2052, Australia

Edited by J. G. Seidman, Harvard Medical School, Boston, MA, and approved September 13, 2012 (received for review April 19, 2012)

MicroRNAs are dysregulated in a setting of heart disease and have emerged as promising therapeutic targets. MicroRNA-34 family members (miR-34a, -34b, and -34c) are up-regulated in the heart in response to stress. In this study, we assessed whether inhibition of the miR-34 family using an s.c.-delivered seed-targeting 8-mer locked nucleic acid (LNA)-modified antimiR (LNA-antimiR-34) can provide therapeutic benefit in mice with preexisting pathological cardiac remodeling and dysfunction due to myocardial infarction (MI) or pressure overload via transverse aortic constriction (TAC). An additional cohort of mice subjected to MI was given LNA-antimiR-34a (15-mer) to inhibit miR-34a alone as a comparison for LNA-antimiR-34. LNA-antimiR-34 (8-mer) efficiently silenced all three miR-34 family members in both cardiac stress models and attenuated cardiac remodeling and atrial enlargement. In contrast, inhibition of miR-34a alone with LNA-antimiR-34a (15-mer) provided no benefit in the MI model. In mice subjected to pressure overload, LNA-antimiR-34 improved systolic function and attenuated lung congestion, associated with reduced cardiac fibrosis, increased angiogenesis, increased Akt activity, decreased atrial natriuretic peptide gene expression, and maintenance of sarcoplasmic reticulum Ca^{2+} ATPase gene expression. Improved outcome in LNA-antimiR-34–treated MI and TAC mice was accompanied by up-regulation of several direct miR-34 targets, including vascular endothelial growth factors, vinculin, protein *O*-fucosyltranferase 1, Notch1, and semaphorin 4B. Our results provide evidence that silencing of the entire miR-34 family can protect the heart against pathological cardiac remodeling and improve function. Furthermore, these data underscore the utility of seed-targeting 8-mer LNA-antimiRs in the development of new therapeutic approaches for pharmacologic inhibition of disease-implicated miRNA seed families.

heart failure | PI3K | pathological hypertrophy | physiological hypertrophy | cardiomyocyte

The prevalence of symptomatic heart failure is increasing owing to the growing elderly population (1). Existing therapies typically slow, rather than prevent or reverse, the progression of heart failure. Furthermore, therapeutics that are effective often have serious side effects (2). Thus, there is an urgent need for well-tolerated therapies with the ability to significantly attenuate adverse cardiac remodeling and improve function of the failing heart. With rapid advances in understanding of the regulation and roles of small, noncoding RNAs known as microRNAs (miRNAs) in cardiac pathology, and developments in antisense oligonucleotide chemistries, the therapeutic potential of inhibition of miRNAs in cardiac disease settings is considered high (3, 4). miRNAs represent attractive therapeutic targets because they are small (~22 nucleotides) and can be efficiently inhibited in vivo (3, 5). The translation of a miRNA-based therapy from mice (6) to primates (7) and into clinical trials has already been demonstrated with miravirsen, an inhibitor of miR-122 for the treatment of hepatitis C virus infection. Results from a Phase 2a trial indicated that the treatment was well tolerated in patients infected with hepatitis C virus and was associated with continuous and prolonged antiviral activity beyond the period of treatment (8). This finding has sparked enthusiasm and anticipation for the development of other miRNA-based drugs.

Phosphoinositide 3-kinase [PI3K(p110α)] lies downstream of the insulin-like growth factor 1 receptor and is an essential mediator of physiological heart growth, that is, normal postnatal heart growth or heart growth in response to chronic exercise training (9–11). PI3K(p110α) also mediates the cardioprotective properties of exercise (12), and elevated PI3K(p110α) activity protects the heart against insults, including pressure overload, dilated cardiomyopathy, and myocardial infarction (MI) (9, 13–15). We previously reported that miR-34a expression was increased in the mouse heart in a setting of stress (i.e., MI) and suppressed in a setting of protection, owing to transgenic expression of PI3K(p110α) (13). We also observed elevated expression of other members of the miR-34 family (i.e., miR-34b and miR-34c) in mouse hearts after MI (13). Furthermore, expression of miR-34a and/or miR-34 b and c was found to be elevated in cardiac tissue from patients with heart disease (16, 17). Thus, we hypothesized that inhibition of the entire miR-34 family in mice with preexisting cardiac dysfunction would be beneficial and demonstrate greater therapeutic potential compared with inhibition of miR-34a alone.

Several previous studies have examined inhibition of individual miRNAs in the heart using chemically modified antisense oligonucleotides known as antimiRs (15-22 mer) (3, 4). Modifications used to enhance the binding affinity of antimiRs to their cognate miRNAs and to facilitate cellular uptake for in vivo delivery include incorporation of 2′-*O*-methyl, 2′-*O*-methoxyethyl, locked nucleic acid (LNA), 3′ cholesterol conjugation (antagomiRs), and phosphorothioate backbone modification (3, 5, 7, 18, 19). More recently, we described an approach to inhibit entire miRNA families using seed-targeting 8-mer LNA-antimiR oligonucleotides known as tiny LNAs (20). Key advantages of this methodology include the ability to simultaneously knock down entire miRNA families, easy formulation in saline for delivery via multiple routes, negligible off-target effects, and no evidence of toxicity. Collectively, these features make tiny LNAs potentially attractive for development of therapeutic strategies for inhibiting disease-associated miRNA families. We report here that s.c. delivery of an 8-mer LNA-modified antimiR-34 efficiently inhibits the miR-34 family (miR-34a, b, and c), attenuates MI-induced remodeling and dysfunction, and improves cardiac function in a model of pressure overload-induced pathological hypertrophy and dysfunction.

Author contributions: B.C.B., C.E.W., P.G., S.O., S.K., R.C.Y.L., and J.R.M. designed research; B.C.B., X.-M.G., C.E.W., E.J.H.B., Y.K.T., H.K., X.-J.D., and J.R.M. performed research; S.O. and S.K. contributed new reagents/analytic tools; B.C.B., C.E.W., E.J.H.B., Y.K.T., R.C.Y.L., and J.R.M. analyzed data; and B.C.B. and J.R.M. wrote the paper.

Conflict of interest statement: S.O. and S.K. are employees of Santaris Pharma, a clinical-stage biopharmaceutical company that develops RNA-targeted therapeutics.

This article is a PNAS Direct Submission.

[1]X.-M.G. and C.E.W. contributed equally to this work.

[2]To whom correspondence should be addressed. E-mail: Julie.mcmullen@bakeridi.edu.au.

This article contains supporting information online at www.pnas.org/lookup/suppl/doi:10.1073/pnas.1206432109/-/DCSupplemental.

MEDICAL SCIENCES

Results

The main focus of this study was to inhibit the entire miR-34 family in settings of cardiac stress using an 8-mer LNA oligonucleotide complementary to the seed region of the miR-34 family (20). A small cohort of mice was also given a 15-mer LNA-modified antimiR-34a specifically targeting miR-34a, for comparison with the 8-mer LNA. We previously reported that miR-34a was increased in hearts of MI mice compared with sham mice, and that expression was inversely correlated with cardiac function, suggesting that inhibition of miR-34a might be beneficial (13). The microarray dataset from which miR-34a was identified (13) also showed elevated miR-34b in hearts of MI mice compared with sham mice, along with a trend toward an increase in miR-34c, which we validated by quantitative RT-PCR (RT-qPCR) (*SI Appendix*, Fig. S1 *A* and *B*). Thus, we hypothesized that inhibition of the entire miR-34 family would represent a more effective treatment strategy than inhibition of miR-34a alone.

Inhibition of the miR-34 Family, but Not of miR-34a Alone, Attenuates MI-Induced Morphological Changes. In adult control mice, we first demonstrated that administration of a single dose of the 15-mer LNA-antimiR-34a on 3 consecutive days inhibited miR-34a in the heart as early as 1 d after administration, and that miR-34a inhibition persisted for 2 mo after the last dose, compared with hearts from LNA-control treated mice (*SI Appendix*, Fig. S2 *A* and *B*). We next assessed the impact of inhibiting miR-34a alone or the entire miR-34 family in mice with preexisting cardiac dysfunction due to MI. Mice subjected to MI (i.e., permanent occlusion of the left anterior descending coronary artery) or the sham operation were dosed with LNA control (15-mer or 8-mer), LNA-antimiR-34 (8-mer), or LNA-antimiR-34a (15-mer) at 2 d after surgery (*SI Appendix*, Fig. S3*A*). Based on morphological and functional parameters (8 wk post-MI), no differences between the 15-mer and 8-mer LNA control-dosed mice were seen; thus, these groups were combined (*SI Appendix*, Fig. S4). The 15-mer LNA-antimiR-34a and the 8-mer LNA-antimiR-34 antagonized miR-34a in the hearts of MI mice compared with LNA control- dosed mice (Fig. 1 *A* and *B*). The 8-mer LNA-antimiR-34 also inhibited miR-34b and miR-34c (Fig. 1*B*). miR-34b and miR-34c were not significantly inhibited in the 15-mer LNA-antimiR-34a–dosed mice (*SI Appendix*, Fig. S5*A*). However, the high homology among the miR-34 family members could allow cross-hybridization of the 15-mer LNA-antimiR-34a with miR-34b and miR-34c, which likely explains the weak inhibition observed for miR-34b and miR-34c (~60% of that of LNA control; *SI Appendix*, Fig. S5 *A* and *B*).

Mean infarct size assessed at dissection was similar in LNA control-treated, LNA-antimiR-34–treated, and LNA-antimiR-34a–treated MI mice (28.7%, 26.1%, and 28.9%, respectively) (*SI Appendix*, Table S1). At 8 wk post-MI, LNA-control treated MI mice displayed significant pathology, including increased heart weight (HW)/tibia length (TL) ratio (Fig. 1*C*), a trend toward an increased lung weight (LW)/TL ratio (Fig. 1*D*; $P = 0.09$), and an increased atrial weight (AW)/TL ratio (Fig. 1 *E* and *F*) compared with sham mice. These morphological changes were blunted by the 8-mer LNA-antimiR-34 (Fig. 1 *C*–*E*), but not with the 15-mer LNA-antimiR-34a (*SI Appendix*, Table S1). Of note, neither LNA-antimiR-34 nor LNA-antimiR-34a had an effect on body weight, spleen weight, or kidney weight compared with LNA control-dosed sham or MI mice (*SI Appendix*, Table S1).

Inhibition of miR-34 Attenuates Pathological Left Ventricular Remodeling After MI. At 2 d post-MI, but before LNA administration, mice displayed significant left ventricular (LV) remodeling, including increased LV dimensions and reduced fractional shortening, compared with sham mice (Fig. 1*G* and *SI Appendix*, Table S2). At 8 wk post-MI, fractional shortening decreased further in the LNA-control treated MI mice (Fig. 1*G*), and thinning of the LV walls was seen (Fig. 1*H* and *SI Appendix*, Table S2). Fractional shortening was higher and LV walls were thicker in LNA-antimiR-34–treated MI mice compared with LNA control-dosed MI mice at 8 wk post-MI (Fig. 1 *G* and *H* and *SI Appendix*, Table S2). Of note, fractional shortening was not improved in LNA-antimiR-34a–dosed MI mice (*SI Appendix*, Fig. S6).

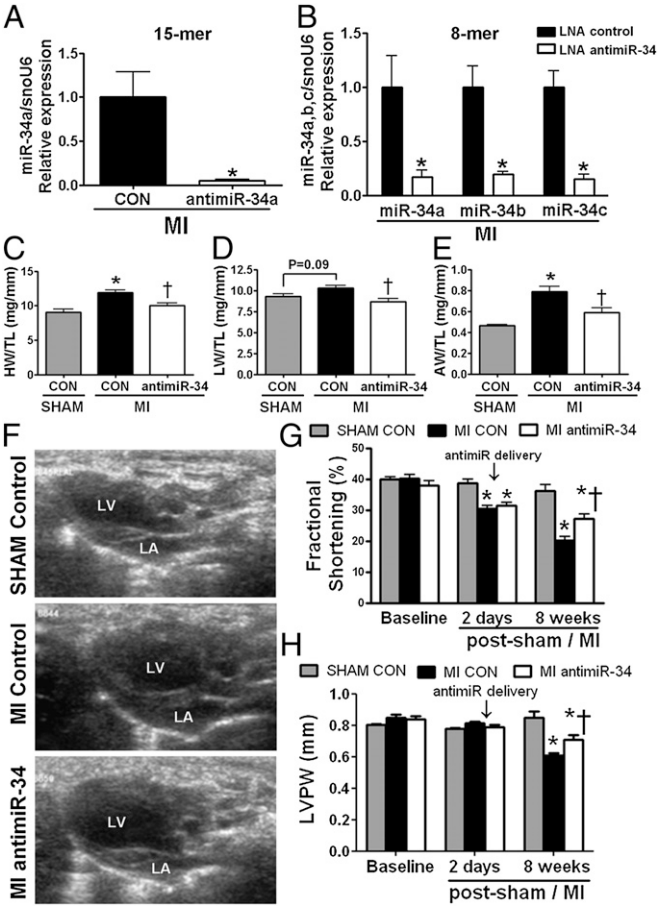

Fig. 1. LNA-antimiR-34 attenuates MI-induced remodeling. (*A*) RT-qPCR showing inhibition of miR-34a in hearts of MI mice dosed with LNA-antimiR-34a vs. LNA control (CON). $n = 3$/group. (*B*) Inhibition of miR-34a, -b, and -c in hearts of LNA-antimiR-34 MI–dosed mice. $^*P \leq 0.05$ vs. LNA control MI. $n = 3$/group. (*C*–*E*) Graphs of HW/TL (*C*), LW/TL (*D*), and AW/TL (*E*). $^*P < 0.05$ vs. sham LNA control; $^\dagger P < 0.05$ vs. MI LNA control. (*F*) Enlarged left atrium (LA; echocardiography:long-axis 2D image) in MI LNA control-dosed mice and attenuation in MI LNA-antimiR-34–dosed mice. (*G* and *H*) Graphs of fractional shortening (*G*) and LV posterior wall thickness (LVPW) (*H*). AntimiR delivery at 2 d post-sham/MI highlighted by arrow. $^*P < 0.05$ vs. sham LNA control and the same group at prior time points; $^\dagger P < 0.05$ vs. MI LNA control at the same time point. $n = 3$/group for sham; $n = 5$/group for MI.

MI is accompanied by an inflammatory response and collagen deposition. Improved outcome in LNA-antimiR-34–treated MI mice was associated with reduced transcription of the inflammatory marker IL-6 in the infarct zone, along with a similar trend in the remote zone (*SI Appendix*, Fig. S7*A*). Collagen 1α1 (*Col1α1*) gene expression was elevated in the infarct zone of all MI groups compared with sham mice and did not differ among groups, although there was a trend toward lower *Col1α1* expression in the remote zone of LNA-antimiR-34–treated MI mice compared with LNA control-treated MI mice (*SI Appendix*, Fig. S7*B*). The α-myosin heavy chain (MHC)/β-MHC ratio (a molecular marker of contractility) was diminished or tended to be reduced in LNA control and LNA-antimiR-34a–treated MI mice, but was not significantly suppressed in LNA-antimiR-34–treated MI mice (*SI Appendix*, Fig. S7*C*).

We next assessed the expression of several validated miR-34a targets that have been implicated in improved outcomes in models of cardiac ischemia and/or cell survival, including cyclin

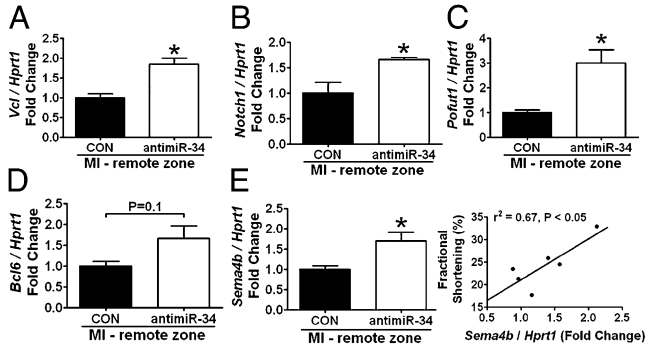

Fig. 2. Up-regulation of miR-34 targets in the remote zone of MI mice treated with LNA-antimiR-34. (*A–E*) RT-qPCR analysis of *Vcl* (*A*), *Notch1* (*B*), *Pofut1* (*C*), *Bcl6* (*D*), and semaphorin 4b (*Sema4b*) (*E, Left*), all standardized to *Hprt1*. **P* < 0.05 vs. LNA control (CON)-dosed MI mice. *n* = 3 per group. (*E, Right*) Correlation of *Sema4b* expression (by RT-qPCR) with fractional shortening in MI mice dosed with LNA-antimiR-34 or LNA control (n = 6).

D1 (*Ccnd1*) (21), silent information regulator 1 (*Sirt1*) (22), and Pnuts (*Ppp1r10*) (23). We found comparable trends toward increased *Ccnd1* in LNA-antimiR-34a–treated and LNA-antimiR-34–treated MI mice (*SI Appendix*, Fig. S7*D*). In contrast, *Sirt1* was increased in LNA-antimiR-34–treated MI mice, but not in LNA-antimiR-34a–treated MI mice (*SI Appendix*, Fig. S7*E*), and a similar trend was apparent for *Ppp1r10* (*SI Appendix*, Fig. S7*F*).

Finally, we measured the expression of predicted targets of the miR-34 family, which also may contribute to the favorable phenotype identified in LNA-antimiR-34–treated MI mice. Expression of vinculin (*Vcl*, essential for cardiomyocyte stability) (24), *Notch1* (critical for cardiac repair after MI) (25), and protein *O*-fucosyltranferase 1 (*Pofut1*, required for functional Notch signaling in vivo) (26) were elevated in the remote zone of LNA-antimiR-34–treated MI mice compared with LNA control-treated MI mice (Fig. 2 *A–C*). *Bcl6* also tended to be elevated (Fig. 2*D*), which protects cardiomyocytes from inflammation (27). We also evaluated semaphorin 4B (*Sema4b*) expression, because in addition to being a miR-34 family target, *Sema4b* is associated with PI3K-mediated cardiac protection in an MI setting (13). *Sema4b* expression was increased in LNA-antimiR-34–treated MI mice compared with LNA control-treated MI mice (Fig. 2*E*, *Left*) and was positively correlated with fractional shortening (Fig. 2*E*, *Right*).

Inhibition of miR-34 Prevents Pressure Overload-Induced LV Remodeling and Improves Cardiac Function. To determine whether inhibition of miR-34 could improve systolic function in a mouse model with preexisting pathological hypertrophy and systolic dysfunction, we subjected mice to pressure overload via transverse aortic constriction (TAC) for 5 wk, followed by 6 wk of treatment with LNA-antimiR-34 (*SI Appendix*, Fig. S3*B*). Before treatment, LV remodeling in response to TAC for 5 wk was confirmed by echocardiography. TAC mice displayed increased LV wall thickness and depressed fractional shortening compared with presurgery values and sham mice (*SI Appendix*, Table S3). Mice were then randomly assigned to receive LNA-antimiR-34 or LNA control for 6 wk.

LNA treatment (LNA control or LNA-antimiR-34) had no impact on body weight during the study period (*SI Appendix*, Table S3). Consistent with our previous observation of increased expression of the miR-34 family in LV of the MI model (*SI Appendix*, Fig. S1) (13), TAC also induced increased expression of miR-34a, b, and c in the heart compared with sham mice (Fig. 3*A*; LNA control TAC vs. LNA control sham). The miR-34 family was antagonized in the hearts of both sham and TAC mice given 8-mer LNA-antimiR-34, as assessed by RT-qPCR (Fig. 3*A*). We also

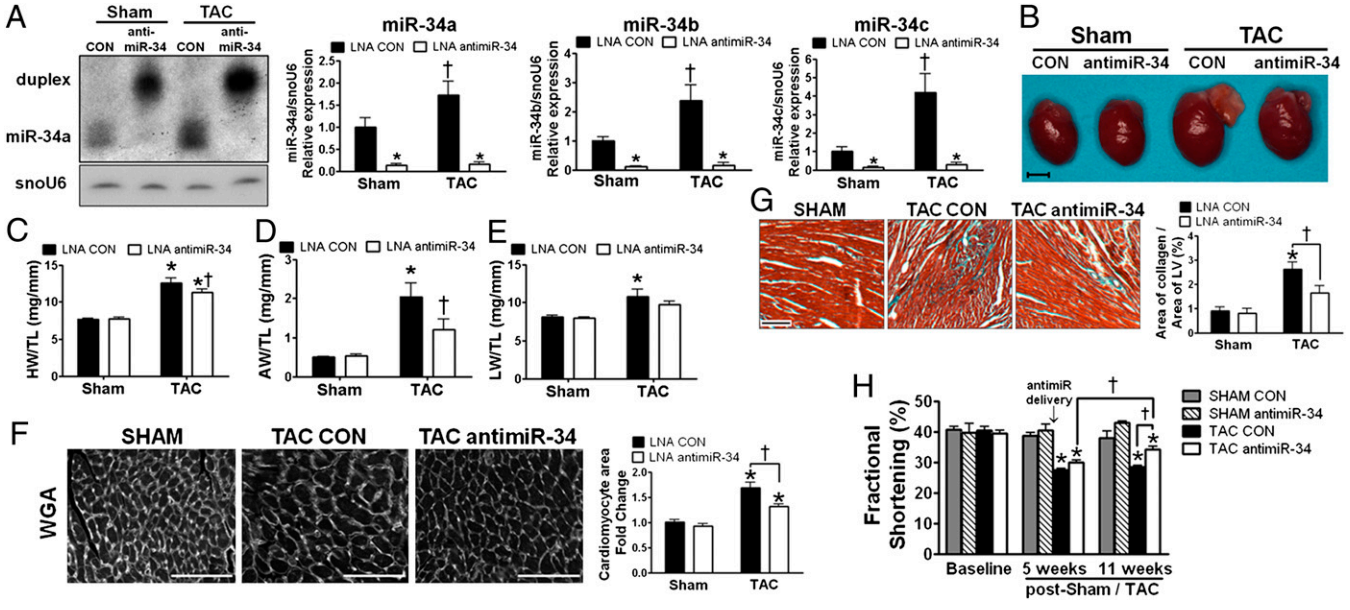

Fig 3. LNA-antimiR-34 inhibits pathological cardiac remodeling and improves systolic function in mice with established cardiac dysfunction due to TAC. (*A*) (*Left*) Northern blot of miR-34a and snoU6 in hearts of sham and TAC mice at 6 wk postadministration with LNA control (CON) or LNA-antimiR-34. The slower-migrating miR-34a:LNA-antimiR-34 band suggests that LNA-antimiR-34 sequesters miR-34a in a stable heteroduplex. (*Right*) Quantification of miR-34a, b, and c relative to snoU6 by RT-qPCR. *n* = 3/group. **P* < 0.05 vs. LNA control from the same group; †*P* < 0.05 vs. LNA control sham. (*B*) Heart photos. (Scale bar: 2.5 mm.) (*C–E*) Graphs of HW/TL (*C*), AW/TL (*D*), and LW/TL (*E*). *n* = 6–9/group. **P* < 0.05 vs. sham with the same treatment; †*P* ≤ 0.05 vs. TAC LNA control. (*F* and *G*) LV cross-sections stained with wheat germ agglutinin (WGA). (*F*, *Left*) or Masson's trichrome (*G*, *Left*) from sham (LNA control) and TAC mice, and quantification of cell area and fibrosis, respectively (*Right*). *n* = 3/group for sham; *n* = 4–6/group for TAC. **P* < 0.05 vs. sham with the same treatment; †*P* ≤ 0.05. (Scale bar: 100 μM in *F*; 50 μM in *G*.) (*H*) Quantification of fractional shortening at baseline (presurgery), 5 wk post-TAC/sham (before LNA oligonucleotides), and 6 wk posttreatment (11 wk postsurgery). *n* = 3/group for sham; *n* = 6–9/group for TAC. AntimiR delivery at wk 5 postsham/TAC is highlighted by the arrow. **P* < 0.05 vs. baseline of the same group and LNA control sham at the same time point; †*P* < 0.05.

assessed inhibition of miR-34a by Northern blot analysis (Fig. 3*A*). Detection of a shifted miR-34a:LNA-antimiR-34 band on Northern blots implies that LNA-antimiR-34 sequesters miR-34a in a stable heteroduplex, thereby inhibiting its function.

LNA control-treated TAC mice developed hypertrophy (increased HW/TL; Fig. 3 *B* and *C*), atrial enlargement (increased AW/TL; Fig. 3 *B* and *D*), and lung congestion (Fig. 3*E*). In contrast, each of these parameters was blunted and/or not significantly elevated (vs. sham) in LNA-antimiR-34–treated TAC mice (Fig. 3 *C*–*E*). LNA-antimiR-34 had no effect on kidney weight (*SI Appendix*, Table S4). The increased heart size in LNA control-treated TAC mice was associated with increased cardiomyocyte size and fibrosis (Fig. 3 *F* and *G*), which were attenuated in LNA-antimiR-34–treated mice.

Fractional shortening decreased by ~30% after 5 wk of pressure overload, associated with an increase in LV end-systolic dimension (Fig. 3 *H* and *SI Appendix*, Table S3). At 6 wk after LNA administration, there was no difference in fractional shortening in LNA control-treated TAC mice compared with pretreatment values at 5 wk after TAC (Fig. 3*H*). In contrast, LNA-antimiR-34 treatment was associated with increased fractional shortening in TAC-treated mice that was significantly improved compared with the same mice at 5 wk after TAC and in LNA-control treated TAC mice at 11 wk after TAC (Fig. 3*H* and *SI Appendix*, Fig. S8).

Inhibition of miR-34 in TAC Mice Is Associated with an Improved Cardiac Molecular Signature, Up-Regulation of miR-34 Targets, and Increased Angiogenesis and Vinculin. Cardiac dysfunction in LNA control-treated TAC mice was accompanied by increased expression of atrial natriuretic peptide (*Anp*; Fig. 4*A*) and *βMHC* (Fig. 4*B*), and decreased sarcoplasmic reticulum Ca^{2+} ATPase (*Serca2a*; Fig. 4*A*). Improved cardiac function in LNA-antimiR-34 treated TAC mice was associated with reduced *Anp* expression, more favorable *Serca2a* expression (Fig. 4*A*), and a higher *αMHC*/*βMHC* ratio (Fig. 4*B*). The phosphorylation of Akt was also elevated in hearts from LNA-antimiR-34 treated TAC mice (Fig. 4*C*).

To investigate the mechanisms by which LNA-antimiR-34 treatment might improve cardiac function in a setting of TAC, we measured the expression of several miR-34 family targets, including VEGFs, POFUT1, and VCL. VEGF-A and VEGF-B have cardioprotective properties (28, 29) and are experimentally validated targets of miR-34 family members (30, 31). In the present study, protein expression of VEGF-A was increased in the hearts of LNA-antimiR-34–treated TAC mice compared with LNA control-treated TAC mice, and a trend toward increased VEGF-B protein expression accompanied by significantly increased *Vegfb* transcription was also seen (Fig. 4*D*). Increased VEGF expression in the hearts of LNA-antimiR-34–treated TAC mice was associated with increased capillary density (Fig. 4*E*). There was a trend toward increased POFUT1 protein expression in LNA-antimiR-34–treated TAC mice that was associated with increased gene transcription (*SI Appendix*, Fig. S9 *A* and *B*). As seen in the MI model, vinculin was elevated in hearts from TAC mice treated with LNA-antimiR-34 (Fig. 4*D*). The intensity of vinculin staining appeared to be reduced at the intercalated disks in myocytes from LNA control-treated TAC mice, but not in LNA-antimiR-34–treated mice, compared with sham mice (Fig. 4*F*).

Vinculin, Sema4b, Pofut1, and Bcl6 Are Targets of the miR-34 Family. Vinculin, Sema4b, Pofut1, and Bcl6 were predicted conserved targets of the miR-34 family in mouse, rat, human, and chimpanzee using TargetScan 6.2 (Fig. 5*A* and *SI Appendix*, Fig. S10). To assess whether miR-34a, b, and c directly bind the 3′ UTR of each predicted target mRNA, we performed luciferase reporter assays in HEK 293T cells and the cardiomyoblast H9c2 cell line (Fig. 5*B* and *SI Appendix*, Fig. S10). Overexpression of miR-34a, b, and c inhibited luciferase activity of reporter constructs containing the 3′ UTR segment of vinculin, Sema4b, Pofut1, or Bcl6. Importantly, luciferase activity was not affected by noncoding RNAs that are not predicted to target the 3′ UTRs of these genes (miR-Ctrl; Fig. 5*B* and *SI Appendix*, Fig. S10), demonstrating specificity of the miR-34 family in targeting the seed region of each 3′ UTR. These data, together with the up-regulation of these targets in hearts from LNA-antimiR-34–treated TAC or MI mice, suggest that vinculin, Sema4b, Pofut1, and Bcl6 are bona fide targets of miR-34a, b, and c.

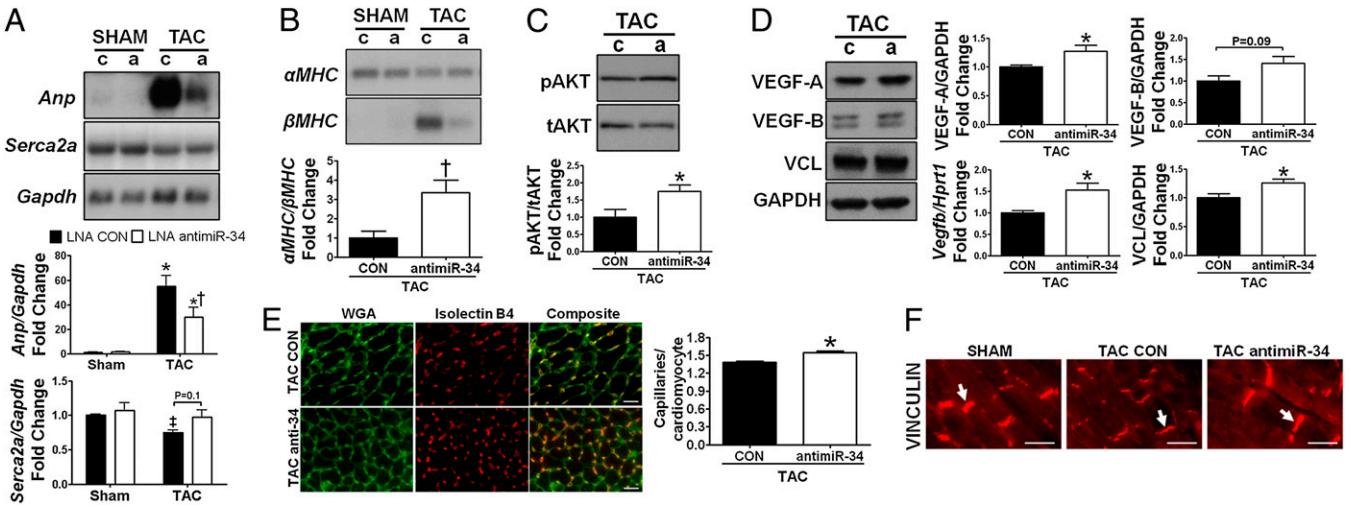

Fig. 4. LNA-antimiR-34 treatment is associated with a more favorable cardiac molecular profile in TAC mice, regulates miR-34 targets, and increases angiogenesis. (*A* and *B*) Northern blots and quantification of *Anp* and *Serca2a* relative to *Gapdh* and *αMHC* relative to *βMHC* in sham and TAC mice dosed with LNA control (CON; c) or LNA-antimiR-34 (a). *βMHC* was not detected in sham mice. $n = 3$–4 for sham mice; $n = 4$–8 for TAC mice. $^{*}P < 0.05$ vs. both sham groups; $^{\dagger}P < 0.05$ vs. TAC LNA control; $^{\ddagger}P < 0.05$ vs. sham LNA control (unpaired *t* test). (*C* and *D*) Western blots and quantification of pAKT relative to tAKT and VEGF-A, VEGF-B, and VCL relative to GAPDH in hearts from TAC mice dosed with LNA control (c) or LNA-antimiR-34 (a). RT-qPCR analysis of *Vegfb* standardized to *Hprt1*. $n = 3$–4 for LNA control TAC mice; $n = 4$–5 for LNA-antimiR-34 TAC mice. $^{*}P < 0.05$ vs. TAC LNA control. (*E*) (*Left*) Capillary density in ventricular sections from TAC mice. Wheat germ agglutinin (WGA) stains myocyte membranes (green), and isolectin B4 stains capillaries (red). (Scale bar: 20 μm.) (*Right*) Quantification ($n = 3$/group). $^{*}P < 0.05$ vs. TAC LNA control. (*F*) Representative images of vinculin staining in hearts from sham and TAC. White arrows highlight intercalated disks. $n = 3$–4 hearts stained/group. (Scale bar: 20 μm.)

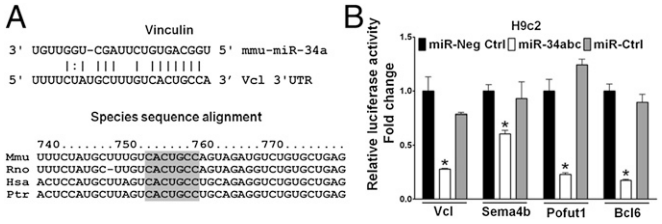

Fig. 5. Vinculin, Sema4b, Pofut1, and Bcl6 are targets of miR-34a, -b, and -c. (*A*) Sequence alignment of miR-34a and the 3′ UTR of Vcl and the miR-34a, -b, and -c seed match sites (gray shaded) within the 3′ UTRs showing conservation among species: Mmu, mouse; Rno, rat; Hsa, human; Ptr, pan troglodytes (chimpanzee). (*B*) Luciferase reporter assays for the 3′ UTRs of Vcl, Sema4b, Pofut1, and Bcl6 in H9c2 cells cotransfected with a negative control (miR-Neg Ctrl); miR-34a, -b, and -c; or a control oligonucleotide (miR-Ctrl: miR-210, miR-27a, or miR-24-1-5p). *$P < 0.05$ relative to controls. Data are presented as the ratio of 3′ UTR luciferase activity to β-gal expression and are representative of four or five independent experiments.

Chronic Administration of LNA-AntimiR-34 Has No Adverse Effects on Tissue Morphology. In vivo delivered antimiRs are known to accumulate in the liver and kidney, and genetic manipulation of the miR-34 family in bone during embryogenesis has been shown to regulate osteoblast proliferation and differentiation (32). In the present study, LNA-antimiR administration had no notable effect on tissues other than the heart, based on weight or morphology at dissection (*SI Appendix*, Tables S1 and S4). To investigate this further, histological assessment was performed in tissues from adult control mice dosed with LNA-antimiR-34. Expression of miR-34a, b, and c were significantly lower or tended to be lower in heart, kidney, liver, and bone from LNA-antimiR-34–treated mice compared with LNA control-treated mice (*SI Appendix*, Fig. S11*A*). Histological analysis revealed no evidence of morphological disarray, inflammation, or toxicity, as well as no impact on osteoblast proliferation and differentiation (*SI Appendix*, Fig. S11*B*).

Discussion

The present study has produced four major findings. First, the miR-34 family was efficiently and chronically silenced using an s.c.-delivered seed-targeting 8-mer LNA. Second, inhibition of the miR-34 family, but not of miR-34a alone, inhibited MI-induced LV remodeling and atrial enlargement, highlighting the therapeutic potential of targeting an entire family. Third, inhibition of the miR-34 family improved systolic function in mice with preexisting pathological hypertrophy and dysfunction due to chronic pressure overload. Fourth, we experimentally validated four miR-34 targets (vinculin, Sema4b, Pofut1 and Bcl6), which were up-regulated and associated with cardiac protection in LNA-antimiR-34–treated TAC and/or MI mice. Also of importance, treatment with LNA-antimiR-34 was not associated with any evidence of morphological disarray, inflammation, or toxicity in the heart, kidney, liver, or bone.

Here we report on the therapeutic inhibition of an entire miRNA seed family in models with established cardiac dysfunction. Previous studies used single or multiple antimiRs (15-22 mer) to inhibit one or more miRNA family members, respectively, in cardiac stress models (4, 33, 34). A recent study also described i.v. delivery of tiny LNA 15b (8-mer, targeting the miR-15 family) in mice at the onset of reperfusion after acute ischemia (75 min), which was associated with reduced infarct size and improved ejection fraction at 2 wk later; however, the tiny LNA 15b and the 16-mer antimiR-15b were not directly compared in that model (35). To our knowledge, the present study is unique in administering an 8-mer LNA-antimiR s.c. against a seed family in mouse models with preexisting cardiac dysfunction and significant pathological remodeling from exposure to chronic cardiac insults (i.e., pressure overload for 5 wk or MI for 2 d, with similar infarct sizes). Furthermore, we directly compared the 8-mer LNA-antimiR-34 and 15-mer LNA-antimiR-34a in the MI model. Our findings demonstrate that administration of a single 8-mer LNA-antimiR can inhibit the entire miR-34 family and provide a benefit in two severe models of cardiac stress with preexisting systolic dysfunction.

The number of new cardiovascular drugs entering the market has been low, in part because many agents under development have not demonstrated clear patient benefits in efficacy over the current standard of care (3). The limited translation of promising approaches identified in basic research laboratories may be due, at least in part, to experimental designs that manipulate genes or deliver therapeutic agents just before or simultaneously with cardiac insults, as opposed to settings of established pathology. Because patients typically seek medical advice once symptoms are present or after an event such as a heart attack, we designed experiments to assess the potential benefit of inhibiting the miR-34 family in two cardiac stress models with significant preexisting LV remodeling and cardiac dysfunction. In the MI study, LNA-antimiR-34 was unable to completely prevent LV remodeling over the 8-wk study period post-MI. However, LNA-antimiR-34–treated MI mice had smaller LV dimensions, increased LV wall thicknesses, and better systolic function compared with LNA control-treated MI mice. Furthermore, MI mice given LNA-antimiR-34 had lower heart, lung, and atrial weights compared with those given LNA control. Of note, the 15-mer LNA-antimiR-34a provided no significant benefit in the MI setting. Our previous work and present results demonstrate increased miR-34b and miR-34c expression in the heart in MI and pressure overload settings. This likely explains why pharmacologic inhibition of the miR-34 family was more effective than inhibition of miR-34a alone. Of note, Dimmeler et al. (23) reported that inhibition of miR-34a was effective in improving ejection fraction in an acute MI setting. Differences between the current study and Dimmeler et al. (23) include the model of MI (acute vs. chronic), time of administration, and type of antimiR delivered (3′-cholesterol-conjugated 2′ *O*-methyl-modified antimiR vs. unconjugated LNA-modified antimiR with a complete phosphorothioate backbone). Whether LNA-antimiR-34a would provide a benefit in the less severe model of acute MI remains to be elucidated. However, given that expression of the entire miR-34 family was elevated in an MI setting, we hypothesize that inhibition of the entire miR-34 family would provide a better therapeutic approach.

Improved systolic function in LNA-antimiR-34–treated TAC mice was associated with reduced fibrosis, increased capillary density, increased cardiac Akt activation, lower *Anp* expression, elevated αMHC/βMHC ratio, and better preserved *Serca2a* gene expression. Fig. 6 illustrates possible mechanisms by which inhibition of the miR-34 family could provide cardiac protection in the TAC and MI models based on regulation of previously validated miR-34 family targets, including VEGFs (30, 31), and targets that we have experimentally validated in the present study (vinculin, Pofut1, Sema4b, and Bcl6). VEGF-A is critical to increasing capillary density, and the reduced coronary angiogenesis in cardiac stress models contributes to the transition to heart failure (29). Vinculin is necessary for the preservation of cardiac contractile and electrical function, and it regulates the expression

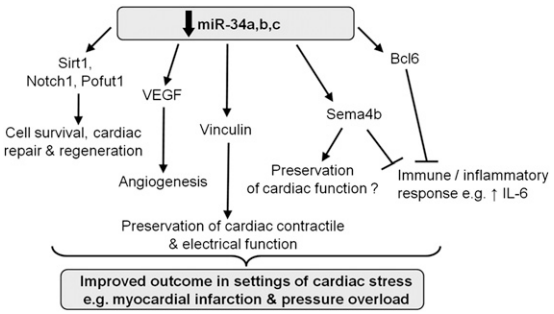

Fig. 6. Potential mechanisms by which inhibition of miR-34a, -b, and -c could mediate protection in settings of cardiac stress.

of proteins residing at the intercalated disk (24). Pofut1 is essential for functional Notch signaling, and heart-specific Pofut1 KO embryos display cardiac defects (26). Notch 1 (a validated target of miR-34a) has been implicated as an important mediator of cardiac repair and regeneration after MI (25). Bcl6 is known to protect mature cardiomyocytes from inflammation (27), and Sema4b has been shown to inhibit IL-6 production by basophils (36). Sema4b was also positively correlated with systolic function in an MI setting (Fig. 2*E*). miRNAs have many target genes, and the present study does not delineate the contribution of identified up-regulated targets in LNA-antimiR-34–treated mice mediating protection. Future in vivo studies incorporating KO models of these targets are needed to comprehensively address this question. However, given that many of these targets have been shown to mediate cardioprotection, we believe that up-regulation of these targets is likely to contribute to the protection observed.

Of note, miR-34 family members also have been recognized as tumor suppressor miRNAs. Given that the miR-34 family has been implicated in the p53 tumor suppressor network, and that p53 pathway defects are common features of human cancer (37), miR-34 replacement therapy is considered a promising therapeutic approach (38). Recent reports demonstrate that inhibition of the miR-34 family does not promote tumorigenesis, supporting the potential for therapeutic suppression of this family as a treatment for heart failure (39). However, because other studies have shown that the miR-34 family may be sufficient to modulate tumor progression (40), future therapeutic approaches might benefit from a targeted approach that can restrict inhibition to the heart. On the other hand, miR-34 replacement in patients with cancer requires caution, because it may make the heart susceptible to dysfunction in a setting of stress.

In summary, our results provide evidence that inhibition of the miR-34 family can improve cardiac function in mice with preexisting pressure overload-induced hypertrophy and systolic dysfunction, and can attenuate pathological remodeling after MI. Furthermore, our data highlight the utility of seed-targeting 8-mer LNA-antimiRs for the pharmacologic inhibition of disease-implicated miRNA seed families. Given that LNA-based therapies have already entered clinical trials, this approach has the potential for translation.

Materials and Methods

Animals. Animal care and experimental procedures were approved by the Alfred Medical Research and Education Precinct's Animal Ethics Committee.

Administration of LNA-AntimiR Oligonucleotides to Control Mice and Cardiac Stress Models. Details of synthesis of LNA-antimiR-34a (15-mer), LNA-antimiR-34 (8-mer), and LNA-control sequences, as well as delivery of LNA-antimiR oligonucleotides in control adult mice and cardiac stress models (MI and TAC), are provided in *SI Appendix*. Details of luciferase assays and histological, molecular, and statistical analyses are also provided in *SI Appendix*.

ACKNOWLEDGMENTS. We thank Dr. P. Kantharidis for advice with the luciferase assays and N. Jennings for assistance with echocardiography. This study was funded by National Health and Medical Research Council Project Grants 586603 (to J.R.M. and R.C.Y.L.) and 586649 (to P.G.) and also supported in part by the Victorian Government's Operational Infrastructure Support Program. X.-J.D. and J.R.M. are National Health and Medical Research Council Senior Research Fellows (317808 and 586604). J.R.M., R.C.Y.L., and P.G. are supported by an Australia Research Council Future Fellowship (FT0001657), a University of New South Wales Vice Chancellor Research Fellowship, and a Pfizer Australia Senior Research Fellowship, respectively.

1. Cubbon RM, et al. (2011) Changing characteristics and mode of death associated with chronic heart failure caused by left ventricular systolic dysfunction: A study across therapeutic eras. *Circ Heart Fail* 4(4):396–403.
2. McMurray JJ (2010) Clinical practice: Systolic heart failure. *N Engl J Med* 362(3):228–238.
3. van Rooij E, Purcell AL, Levin AA (2012) Developing microRNA therapeutics. *Circ Res* 110(3):496–507.
4. Small EM, Olson EN (2011) Pervasive roles of microRNAs in cardiovascular biology. *Nature* 469(7330):336–342.
5. Bernardo BC, Charchar FJ, Lin RC, McMullen JR (2012) A microRNA guide for clinicians and basic scientists: Background and experimental techniques. *Heart Lung Circ* 21(3):131–142.
6. Elmén J, et al. (2008) Antagonism of microRNA-122 in mice by systemically administered LNA-antimiR leads to up-regulation of a large set of predicted target mRNAs in the liver. *Nucleic Acids Res* 36(4):1153–1162.
7. Elmén J, et al. (2008) LNA-mediated microRNA silencing in non-human primates. *Nature* 452(7189):896–899.
8. Stenvang J, Petri A, Lindow M, Obad S, Kauppinen S (2012) Inhibition of microRNA function by antimiR oligonucleotides. *Silence* 3(1):1.
9. McMullen JR, et al. (2003) Phosphoinositide 3-kinase(p110alpha) plays a critical role for the induction of physiological, but not pathological, cardiac hypertrophy. *Proc Natl Acad Sci USA* 100(21):12355–12360.
10. McMullen JR, et al. (2004) The insulin-like growth factor 1 receptor induces physiological heart growth via the phosphoinositide 3-kinase(p110alpha) pathway. *J Biol Chem* 279(6):4782–4793.
11. Bernardo BC, Weeks KL, Pretorius L, McMullen JR (2010) Molecular distinction between physiological and pathological cardiac hypertrophy: Experimental findings and therapeutic strategies. *Pharmacol Ther* 128(1):191–227.
12. Weeks KL, et al. (2012) Phosphoinositide 3-kinase p110α is a master regulator of exercise-induced cardioprotection and PI3K gene therapy rescues cardiac dysfunction. *Circ Heart Fail* 5(4):523–534.
13. Lin RC, et al. (2010) PI3K(p110 alpha) protects against myocardial infarction-induced heart failure: Identification of PI3K-regulated miRNA and mRNA. *Arterioscler Thromb Vasc Biol* 30(4):724–732.
14. McMullen JR, et al. (2007) Protective effects of exercise and phosphoinositide 3-kinase (p110alpha) signaling in dilated and hypertrophic cardiomyopathy. *Proc Natl Acad Sci USA* 104(2):612–617.
15. Pretorius L, et al. (2009) Reduced phosphoinositide 3-kinase (p110alpha) activation increases the susceptibility to atrial fibrillation. *Am J Pathol* 175(3):998–1009.
16. Thum T, et al. (2007) MicroRNAs in the human heart: A clue to fetal gene reprogramming in heart failure. *Circulation* 116(3):258–267.
17. Greco S, et al. (2012) MicroRNA dysregulation in diabetic ischemic heart failure patients. *Diabetes* 61(6):1633–1641.
18. Krützfeldt J, et al. (2005) Silencing of microRNAs in vivo with "antagomirs." *Nature* 438(7068):685–689.
19. Davis S, et al. (2009) Potent inhibition of microRNA in vivo without degradation. *Nucleic Acids Res* 37(1):70–77.
20. Obad S, et al. (2011) Silencing of microRNA families by seed-targeting tiny LNAs. *Nat Genet* 43(4):371–378.
21. Tamamori-Adachi M, et al. (2008) Cardiomyocyte proliferation and protection against post-myocardial infarction heart failure by cyclin D1 and Skp2 ubiquitin ligase. *Cardiovasc Res* 80(2):181–190.
22. Hsu CP, et al. (2010) Silent information regulator 1 protects the heart from ischemia/reperfusion. *Circulation* 122(21):2170–2182.
23. Boon RA, et al. (2010) Inhibition of the age-induced microRNA-34 improves recovery after AMI in mice. *Circulation* 122(21):A14023.
24. Zemljic-Harpf AE, et al. (2007) Cardiac myocyte-specific excision of the vinculin gene disrupts cellular junctions, causing sudden death or dilated cardiomyopathy. *Mol Cell Biol* 27(21):7522–7537.
25. Li Y, Hiroi Y, Liao JK (2010) Notch signaling as an important mediator of cardiac repair and regeneration after myocardial infarction. *Trends Cardiovasc Med* 20(7):228–231.
26. Okamura Y, Saga Y (2008) Pofut1 is required for the proper localization of the Notch receptor during mouse development. *Mech Dev* 125(8):663–673.
27. Yoshida T, et al. (1999) The role of Bcl6 in mature cardiac myocytes. *Cardiovasc Res* 42 (3):670–679.
28. Lähteenvuo JE, et al. (2009) Vascular endothelial growth factor-B induces myocardium-specific angiogenesis and arteriogenesis via vascular endothelial growth factor receptor-1- and neuropilin receptor-1-dependent mechanisms. *Circulation* 119(6):845–856.
29. Shiojima I, et al. (2005) Disruption of coordinated cardiac hypertrophy and angiogenesis contributes to the transition to heart failure. *J Clin Invest* 115(8):2108–2118.
30. Nalls D, Tang SN, Rodova M, Srivastava RK, Shankar S (2011) Targeting epigenetic regulation of miR-34a for treatment of pancreatic cancer by inhibition of pancreatic cancer stem cells. *PLoS ONE* 6(8):e24099.
31. Ye W, et al. (2008) The effect of central loops in miRNA:MRE duplexes on the efficiency of miRNA-mediated gene regulation. *PLoS ONE* 3(3):e1719.
32. Wei J, et al. (2012) miR-34s inhibit osteoblast proliferation and differentiation in the mouse by targeting SATB2. *J Cell Biol* 197(4):509–521.
33. Porrello ER, et al. (2011) MiR-15 family regulates postnatal mitotic arrest of cardiomyocytes. *Circ Res* 109(6):670–679.
34. Montgomery RL, et al. (2011) Therapeutic inhibition of miR-208a improves cardiac function and survival during heart failure. *Circulation* 124(14):1537–1547.
35. Hullinger TG, et al. (2012) Inhibition of miR-15 protects against cardiac ischemic injury. *Circ Res* 110(1):71–81.
36. Nakagawa Y, et al. (2011) Identification of semaphorin 4B as a negative regulator of basophil-mediated immune responses. *J Immunol* 186(5):2881–2888.
37. Vogelstein B, Lane D, Levine AJ (2000) Surfing the p53 network. *Nature* 408(6810): 307–310.
38. Bader AG, Brown D, Winkler M (2010) The promise of microRNA replacement therapy. *Cancer Res* 70(18):7027–7030.
39. Concepcion CP, et al. (2012) Intact p53-dependent responses in miR-34-deficient mice. *PLoS Genet* 8(7):e1002797.
40. Silber J, et al. (2012) miR-34a repression in proneural malignant gliomas upregulates expression of its target PDGFRA and promotes tumorigenesis. *PLoS ONE* 7(3):e33844.